Symmetry **2014**, *6*, 383-395; doi:10.3390/sym6020383

OPEN ACCESS

symmetry

ISSN 2073-8994

www.mdpi.com/journal/symmetry

Review

Hydrodynamic Helical Orientations of Nanofibers in a Vortex

Akihiko Tsuda

Department of Chemistry, Graduate School of Science, Kobe University, 1-1 Rokkodai-cho, Nada-ku, Kobe 657-8501, Japan; E-Mail: tsuda@harbor.kobe-u.ac.jp; Tel./Fax: +81-78-803-5671

Received: 15 April 2014; in revised form: 14 May 2014 / Accepted: 15 May 2014 / Published: 20 May 2014

Abstract: In this review article, I report our recent studies on spectroscopic visualizations of macroscopic helical alignments of nanofibers in vortex flows. Our designed supramolecular nanofibers, formed through self-assemblies of dye molecules, helically align in torsional flows of a vortex generated by mechanical rotary stirring of the sample solutions. The nanofiber, formed through bundling of linear supramolecular polymers, aligns equally in right- and left-handed vortex flows. However, in contrast, a one-handedly twisted nanofiber, formed through helical bundling of the supramolecular polymers, shows unequal helical alignments in these torsional flows. When the helical handedness of the nanofiber matches that of the vortex flow, the nanofiber aligns more efficiently in the flowing fluid. Such phenomena are observed not only with the artificial helical supramolecular nanofibers but also with biological nanofibers such as double-stranded DNA.

Keywords: nanofiber; supramolecular polymer; DNA; vortex; stirring; linear dichroism; helical alignment

---

1. Introduction

Vortexes are recognized as macroscopic chirality elements [1] and one of the possible origins of chiral symmetry breaking in nature [2–12]. Compared with, e.g., rheometric shear flows, vortexes are complex, involving many locally different fluid flows. For example, upon mechanical rotary stirring of a fluid in a cuvette, a tight, torsional flow is generated at the rotary center, while the peripheral part of the vortex involves a loose, spiral flow (Figure 1) [13]. We were prompted to investigate whether these vortex flows can be utilized for controlling the orientations of molecules or molecular assemblies.

Figure 1. Schematic illustrations of (**a**) chiral vortex flows generated upon rotary clockwise (CW) or counterclockwise (CCW) stirring with a magnetic stirring bar; (**b**) a macroscopic helical alignment of multiple fibers in a vortex as light passes during spectroscopy; and (**c**) (*P*)-helical deformation of an elastic fiber at the vortex center.

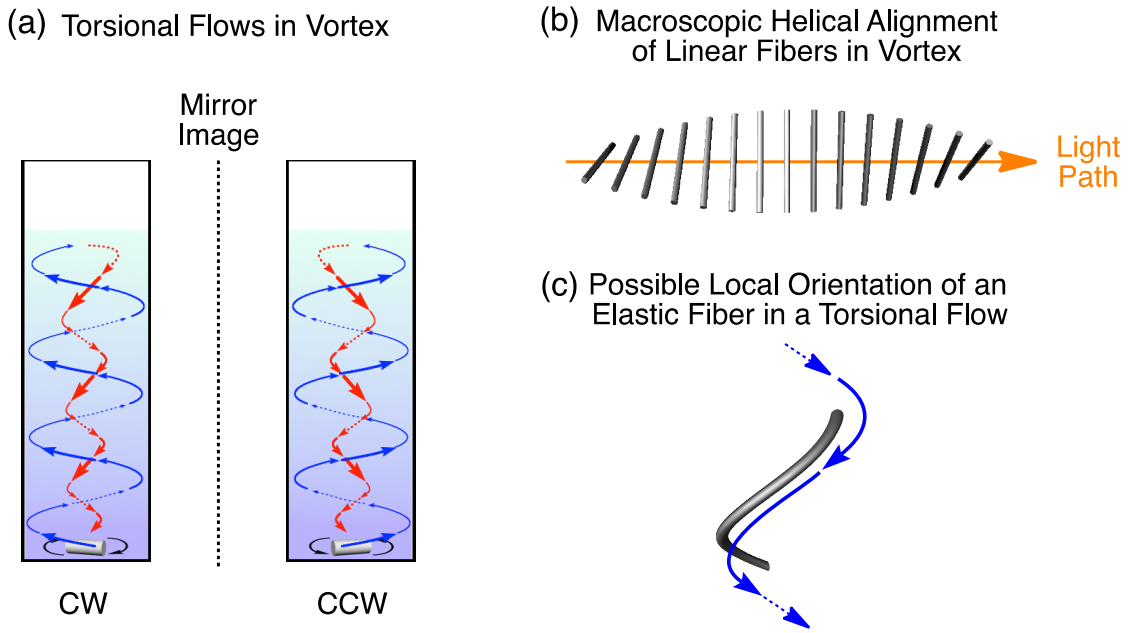

Small molecules rarely orient along the macroscopic flowing direction of solvent molecules because Brownian motions are dominant over hydrodynamic interactions at the molecular level. However, when molecules or molecular assemblies are long enough to average local effects of Brownian motions of the solvent molecules, they begin to react to the fluid flows. In fact, certain nanoscale molecules and molecular assemblies having anisotropic structures are known to sense the shear forces of fluid flows [14–16]. Ribó *et al.* have reported that electrostatic *J*-aggregates of (4-sulfophenyl)porphyrin derivatives, prepared in aqueous media upon rotary stirring, become optically active, and suggested that hydrodynamic selection of either the right- or left-handed helical conformation of the aggregates is responsible [7,8]. The formation of helical ribbons in such a stirred solution has been confirmed [9,17]. However, the hydrodynamic interactions of the aggregates with the fluid have not sufficiently been clarified experimentally. With this in mind, we became interested in the macroscopic physical interactions between nanoscale objects and fluid flows.

In this review article, I report our recent studies on spectroscopic visualizations of macroscopic helical alignments of nanofibers, including supramolecular polymers and biopolymers such as DNA (Figure 1b,c). Linear dichroism (LD) and circular dichroism (CD) spectroscopies allow the visualization of helical alignments in torsional flows of a vortex generated by mechanical rotary stirring of fluids. We initially discovered the helical alignment of a supramolecular nanofiber, composed of a zinc porphyrin derivative bearing dendritic substituents, in the vortex [13,18]. Next, a one-handedly twisted supramolecular nanofiber was found to show unequal LD responses in right- and left-handed vortex flows, owing to unequal helical alignment of the nanofiber [19]. Such phenomena were observed not only in the artificial helical supramolecular nanofibers but also in biological nanofibers such as double-stranded DNA [20].

2. Helical Alignment of a Supramolecular Nanofiber in a Vortex Flow

A supramolecular polymer of zinc porphyrin dendrimer **DP** (Figure 2a) can helically align in a vortex generated by mechanical rotary stirring of a fluid in an optical cell [13,21]. **DP** self-assembles to form a *J*-aggregate in nonpolar solvents by π-stacking interactions and hydrogen bonds involving its carboxylic acid side groups (Figure 2b) [11]. Transmission electron microscopy (TEM) of the benzene solution of **DP** shows nanofibers with 10–20 nm diameters (Figure 2c). A benzene solution of **DP** without stirring is CD silent, but exhibits a CD spectrum upon mechanical rotary stirring (Figure 3b). For example, when stirring in a clockwise direction (CW), the sample solution of **DP** displays intense CD bands at the Soret absorption bands (413, 449, and 455 nm) and weak ones in the Q-band region (530–610 nm) due to *J*-aggregated **DP**. No chiroptical response emerges at the absorption band (430 nm) of non-assembled **DP**. A dip-coated thin film of **DP**, where the nanofibers are oriented preferentially along the dipping direction, can be prepared on a thick glass plate with a benzene solution. When this nanofiber-coated glass plate is laid over another in such a way that their oriented directions are angled by 45°, a distinct chiroptical response appears in the CD spectrum. The observed spectral shape is virtually identical to that observed for the stirred solution of *J*-aggregated **DP**. A spectral inversion takes place by varying the dihedral angle of overlaying from 45° to −45°. These experimental results indicate that the observed CD originates from macroscopic chiral alignments of nanofibers in the vortex flows generated by rotary stirring. However, one must note that the observed CD may originate from not only a true CD signal but also artifactual combinations of linear dichroism (LD), linear birefringence (LB), and circular birefringence (CB) [22]. We have not evaluated their contributions in the observed CD spectra, but Mueller matrix spectroscopy, developed by Ribó *et al.*, may allow their evaluations [23–25].

Linear dichroism (LD) spectroscopy, defined as the difference between absorption of light polarized parallel and polarized perpendicular to an orientation axis ($\Lambda\Delta = A_{//} - A_{\perp}$), gives information on the alignment of macromolecules such as carbon nanotubes and DNA [26–31]. Although the sample solution ([**DP**] = 6.0×10^{-6} M) containing the long nanofibers is LD silent without stirring, it becomes LD active upon rotary stirring (Figure 3c). Since the observed negative and positive signs of LD bands at λ_{max} at 448 and 408 nm, respectively, originate from electronic transitions due to longer and shorter axes of the *J*-aggregated **DP**, respectively (Figure 3c) [32], it can be expected that **DP** nanofibers align perpendicularly to the rotary direction. This result is also supported by the fact that the spectral pattern is the same as that of the dip-coated film sample, placed in such a way that its oriented direction is parallel to the vertical axis of the linearly polarized incident light. The fluidic situations in a vortex, generated by rotary stirring, are locally different. Point-wise LD and CD spectroscopies with optical cells selectively masked at the marginal parts or vertical center show that the LD sign observed through the central slit of the masked cell is identical to that of the entire solution, but the LD spectrum observed through the marginal parts is opposite in sign to the others. These observations suggest that the preferential alignments of the nanofibers flowing at the center and periphery of the vortex are different from one another. The CD response observed through the center part is more intense than that with an unmasked cell, but the response through the marginal parts is much less intense. Considering the obtained experimental results and hydrodynamic model of a vortex generated in a cuvette (Figure 1), the

DP nanofiber reacts in its orientation to the locally different fluid flows of the vortex, and dominantly aligns at the center of the vortex.

Figure 2. Structural formulas of (**a**) dendritic zinc porphyrin **DP**; and (**b**) *J*-aggregated form of hydrogen-bonded supramolecular polymer (nanofiber) of **DP**. DRN represents a dendritic wedge; (**c**) A transmission electron micrograph (TEM) of an air-dried sample of a benzene solution of **DP**.

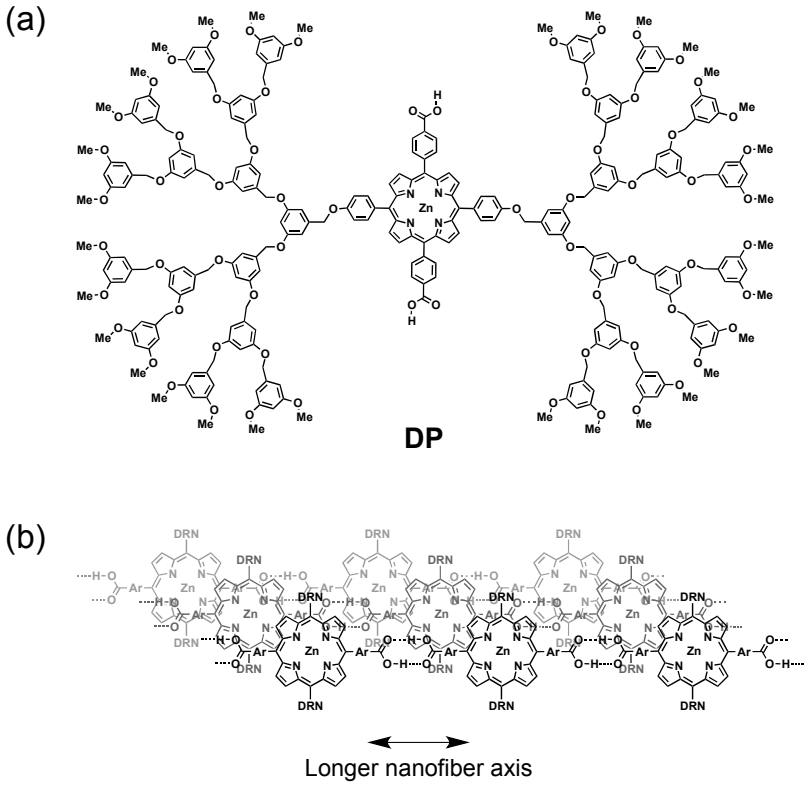

Figure 3. (**a**) Electronic absorption; (**b**) circular dichroism (CD); and (**c**) linear dichroism (LD) spectroscopies of a benzene solution of the nanofibers of **DP** (6.0×10^{-6} M), upon rotary stirring at 1350 rpm in clockwise (blue curves) or counterclockwise (red curves) direction using a ϕ2.0 mm × 5.0 mm Teflon-coated magnetic stirring bar at 20 °C in 10 mm × 10 mm × 40 mm quartz optical cells.

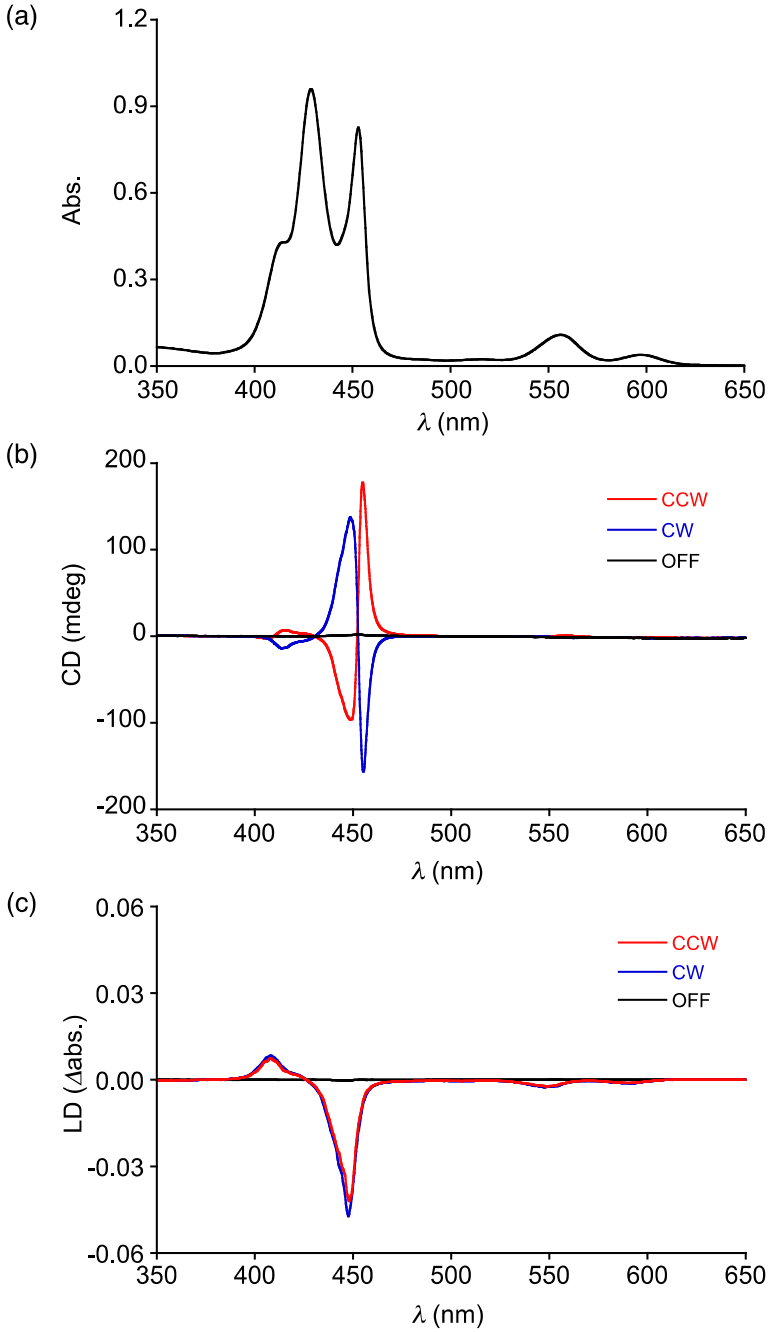

This phenomenon observed with the nanofibers of *J*-aggregated **DP** is known for cholesteric liquid crystalline materials involving a macroscopic helical alignment of mesogenic molecules [33]. However, it is noteworthy that, in our system, such a macroscopic helical alignment occurs in non-constrained fluid media without any assistance from rheometric flows.

3. Unequal Helical Orientations of a One-Handedly Twisted Helical Supramolecular Nanofiber in Right- and Left-Handed Vortex Flows

An anthracene derivative **AN**, bearing *N*-phenyl amide groups with optically active alkyl chains, in *n*-hexane forms one-handedly twisted helical supramolecular nanofibers (Figure 4) [34–36]. The sample solution of the **AN** nanofiber exhibits an induced LD spectrum, whose intensity changes reversibly upon clockwise (CW) and counterclockwise (CCW) stirring of the solution [19]. Frequency-modulation atomic force microscopy (FM-AFM) performed on a HOPG substrate with a solution of self-assembled (*R*)-**AN** in *n*-hexane shows the presence of linear nanofibers (Figure 4c) [37,38]. These nanofibers have twisted structures with right-handed *P*-helicity (Figure 4d), whose direction is in agreement with that expected from the exciton coupled CD [39,40]. **AN** molecules in nonpolar solvents self-assemble through possible multiple intermolecular interactions such as hydrogen bonds of the amide groups, π–π interactions of anthracene components, and Van der Waals interactions of the long alkyl chains to form *J*-aggregated supramolecular nanofibers (Figure 4b) [41].

Figure 4. (**a**) Chemical structures of (*R*)- and (*S*)-**AN**; (**b**) Schematic illustration of a twisted *J*-aggregation of (*R*)-**AN** molecules; (**c**,**d**) Frequency-modulation atomic force microscopy (FM-AFM) images of the (*R*)-**AN** supramolecular nanofibers.

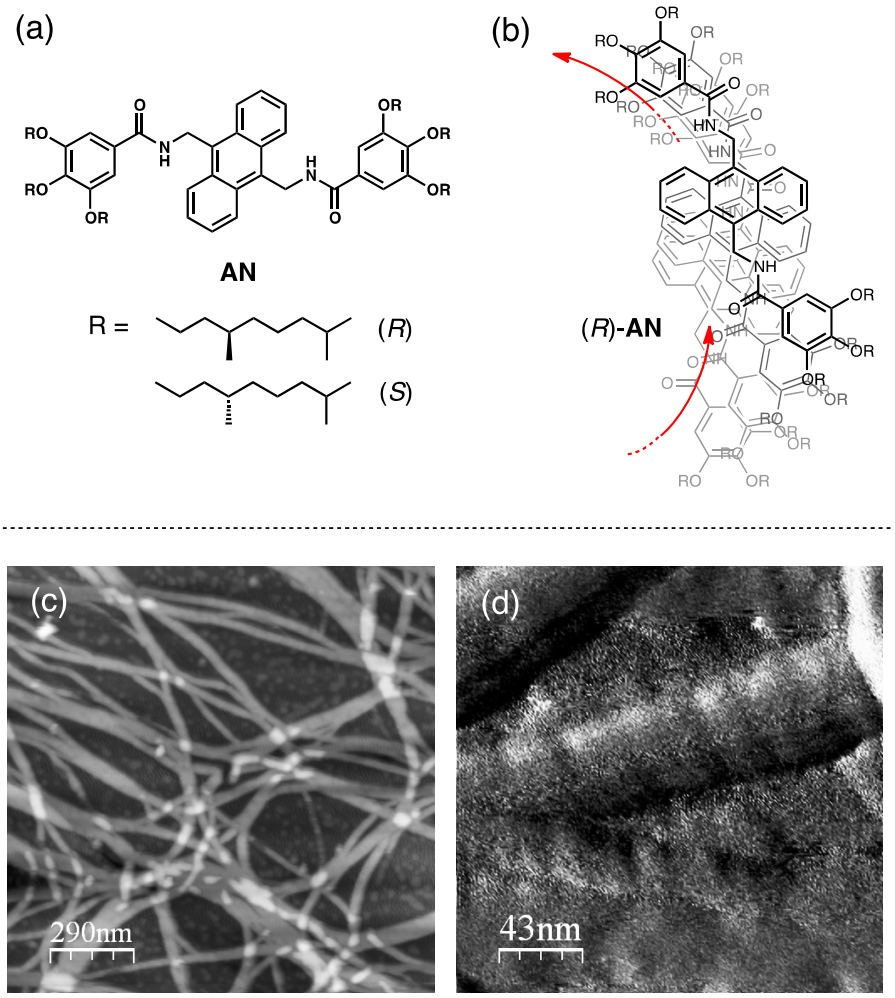

Although the *n*-hexane solution of **AN** without stirring is LD silent, it becomes LD active upon mechanical rotary stirring. The LD intensity observed with the (*R*)-**AN** nanofiber upon CW stirring decreases dramatically when the stirring direction is changed to the opposite CCW direction (Figure 5a). The solution quickly responds to the applied changes in stirring directions. Furthermore, its enantiomer (*S*)-**AN** displays the opposite unequal LD responses for CW and CCW stirrings of the sample solution (Figure 5b). The observed difference of LD intensity originates mainly from the center of the vortex flow. Since the CW and CCW stirrings generate right- and left-handed downward spiral flows, respectively, the larger LD intensity is found to appear when the helical direction of the (*R*)-**AN** nanofiber harmonizes with the torsional flowing direction of the vortex. Chiral hydrodynamic interactions between helical supramolecular nanofibers and torsional flows in the vortex, which have also been suggested in some other studies [9,17], may affect the alignments and assembling behaviors of the **AN** nanofibers in the solution. In dynamic light scattering (DLS) analysis, the *n*-hexane solution of the self-assembled (*R*)-**AN** after CW and CCW stirring for 30 min actually shows different size distributions in the histogram, where the vortex flow having the same helical handedness with that of the supramolecular nanofiber allows formation of a larger assembly.

Figure 5. Unequal helical alignments of one-handedly twisted **AN** nanofibers in the vortex flows. LD spectra of (**a**) (*R*)-**AN** and (**b**) (*S*)-**AN** nanofibers induced upon CW (—) or CCW (—) rotary stirring.

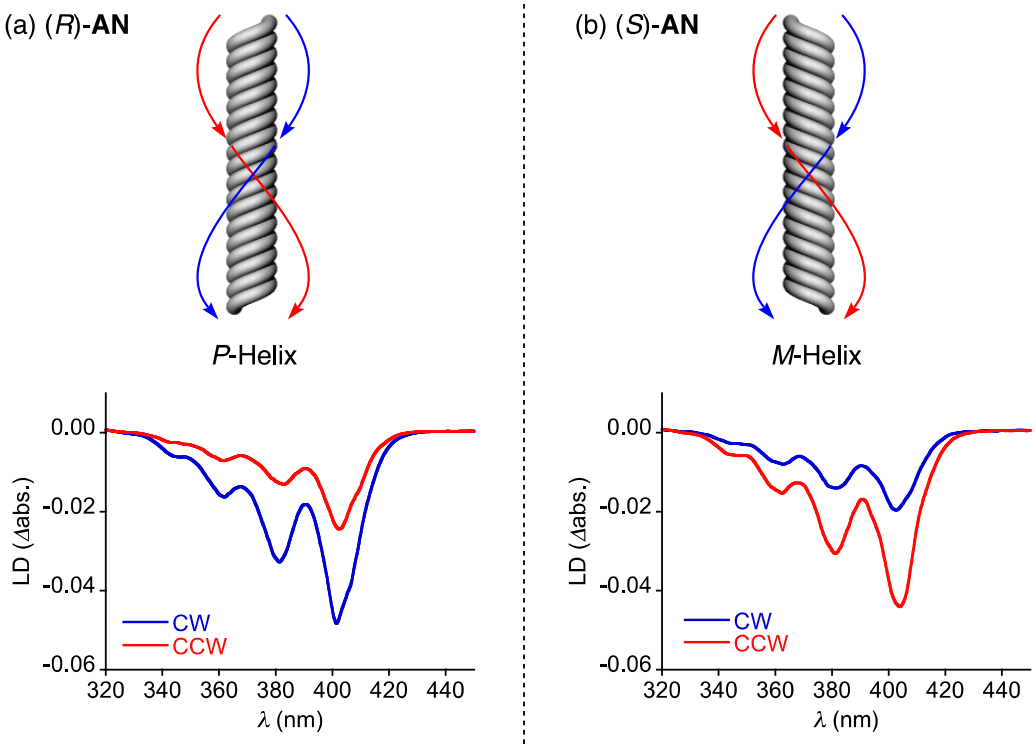

4. Unequal Helical Orientations of a Double-Stranded DNA in Right- and Left-Handed Vortex Flows

From the results obtained from the studies on helical orientations of the twisted supramolecular nanofibers described above, we became interested in the macroscopic chiral hydrodynamic interactions

of biological nanofibers such as DNA [26] with vortex flows. Double-stranded DNA has a right-handed helical structure with a diameter of 2.2–2.6 nm, and can hydrodynamically align and stretch in certain linear fluid flows [42,43]. A wormlike chain model can reasonably account for the elastic behaviors and hydrodynamic interactions of DNA [44]. Strick *et al.* reported the first single-molecule measurements of DNA topology using magnetic tweezers. They measured the extension and force of individual λ-phage DNA molecules and found that positively supercoiled DNA was more difficult to stretch than negatively supercoiled DNA [45]. Other studies have demonstrated experimentally the intrinsic chiral twist elasticity of DNA [46,47]. These studies raise an important question: what happens to DNA in a chiral macroscopic vortex generated by clockwise (CW) or counterclockwise (CCW) stirring? We revealed that DNA molecules in pure water align helically with the spiral flow generated by mechanical rotary stirring in an optical cell, and display strong induced circular dichroism (CD) and linear dichroism (LD) responses [20].

An aqueous solution of salmon testes DNA (5.1×10^{-2} mg/mL), having a linear structure with an average molecular weight of approximately $M_W = 1.3 \times 10^6$ (2000 bp), without stirring exhibits the characteristic CD spectral pattern of DNA with peak maxima at λ_{max} = 247 and 279 nm (Figure 6). However, an entirely different macroscopic CD spectral pattern with a much larger intensity with λ_{max} of 266 nm and an LD spectrum with a positive peak at λ_{max} of 259 nm appear upon mechanical rotary stirring of the sample solution. Clockwise (CW) and counterclockwise (CCW) stirring give mirror-image CD spectral profiles and virtually the same LD profiles with different intensities. The CW stirring of the sample solution in LD spectroscopy always results in larger spectral intensity than CCW stirring, but the differences become negligible upon addition of NaCl or ethidium bromide, which reduce structural elasticity of DNA [48,49]. An increase of ionic strength of the aqueous solvent reduces the mutually repulsive forces of negative charges on the two DNA strands; therefore, the elasticity, higher order structures and the denaturation temperature of the DNA molecules are changed. On the other hand, accommodations of multiple molecules of ethidium bromide (ETB) in the spaces between the base pairs of DNA by unwinding induce local structural changes to the double-stranded DNA (e.g., lengthening and hardening). The relaxed coil may, thus, have larger differences in the chiral twist elasticity for CW and CCW directions than that of rigid DNA. The observed CD and LD responses of the stirred sample solution are also decreased simultaneously as the double-stranded structure denatures at increasing temperatures. Furthermore, these induced CD and LD responses are not observed upon stirring in a solution containing shorter DNA with low molecular weight (approximately $M_W = 0.5 \times 10^5$–1.0×10^5) that may not sense hydrodynamic shear force of fluids beyond Brownian motions of the solvent. The long double-stranded DNA molecules, thus, can be effectively aligned in the vortex flows, and show hydrodynamic preference for a right-handed vortex than for a left-handed vortex. The observed preference is emphasized when using a smaller stirring bar, which can generate a more narrow torsional flow at the center of the vortex. Decreases in the scale gap between the DNA and the torsional flow may enhance the present chiral hydrodynamic interaction. This study suggests that chiral hydrodynamic interactions between asymmetric biomolecules and fluids are important in natural biological systems.

Figure 6. Unequal helical alignments of a double-stranded DNA in the vortex flows. CD (**a**) and LD (**b**) spectra of a solution of salmon testes DNA dissolved in pure water at 5 °C with CW (blue curve) or CCW (red curve) stirring.

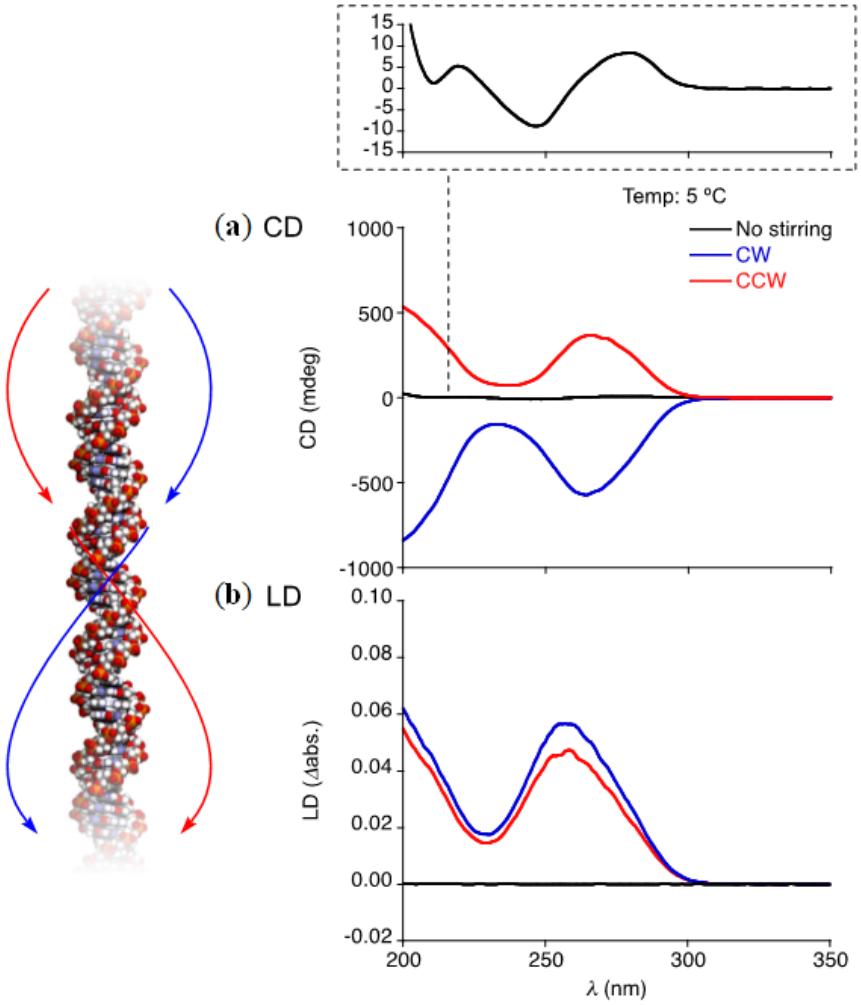

5. Conclusions

In this review article, I have summarized and extended our findings presented in references [13,19,20]. Small molecules do not orient in response to macroscopic fluid flows of solvent molecules, because Brownian motions are dominant over hydrodynamic interactions at the molecular level. However, when molecules or molecular assemblies have fiber structures long enough to average local effects of Brownian motions of the solvent molecules, they orient in fluid flows by sensing weak velocity gradients generated in the flowing fluid and the boundary layer on glass surfaces of the cuvette. CD and LD spectroscopies provide information about chiral orientations of molecules and molecular assemblies, and allow spectroscopic visualizations of helical alignments in the torsional flows of a vortex. Mueller matrix spectroscopy will strongly support to reveal origin of the observed CD spectra. Because we have not observed the same phenomenon with linear conjugated polymers to date, the observed phenomenon may be the characteristic behavior of self-assembled molecular architectures having linear structures. As observed in the shapes of all nanofibers described above, it can be concluded that the bundling of single polymers is essential to cause hydrodynamic alignments of the

nanofibers in the vortex flows. The bundle structure increases structural linearity, rigidity, length, and volume of the nanofiber, and also enhances macroscopic hydrodynamic interactions between the nanofiber and the solvent molecules. In such helical orientations of the nanofibers in the vortex flow, the chiral hydrodynamic interactions between the one-handedly twisted nanofiber and the vortex, including right- or left-handed torsional flows, are unequal in the combinations. The helical nanofibers align more efficiently when the helical handedness matches that of the vortex flows. Additionally, size distribution of the helical supramolecular nanofiber changes upon CW or CCW stirring of the sample solution. A larger assembly forms when the helical handedness of the nanofiber matches that of the vortex flows. The observed chiral hydrodynamic interactions thus also affect dynamic self-assembly of the molecules in the solution. These experimental results that spectroscopically reveal a physical chiral interaction between nanoscale molecules and torsional fluid flows are key information to elucidate the origin of chiral symmetry breaking in nature.

Acknowledgements

I warmly thank all the collaborators and co-workers and, particularly, Takuzo Aida who have greatly contributed to my research in this area.

Conflicts of Interest

The author declares no conflict of interest.

References

1. Hama, F.R.; Nutant, J. Self-induced velocity on a curved vortex. *Phys. Fluids* **1961**, *4*, 28–32.
2. Mason, S.F. Origins of biomolecular handedness. *Nature* **1984**, *311*, 19–23.
3. Link, D.R.; Natale, G.; Shao, R.; Maclennan, J.E.; Clark, N.A.; Körblova, C.E.; Walba, D.M. Spontaneous formation of macroscopic chiral domains in a fluid smectic phase of achiral molecules. *Science* **1997**, *278*, 1924–1927.
4. Pramod, P.A.; Hatwalne, Y.; Madhusudana, N.V. Chiral symmetry breaking in three-dimensional smectic-C liquid-crystal domains. *Phys. Rev. E* **1997**, *56*, 4935–4938.
5. Kondepudi, D.K.; Kaufman, R.J.; Singh, N. Chiral symmetry breaking in sodium chlorate crystallizaton. *Science* **1990**, *250*, 975–976.
6. Kondepudi, D.K.; Laudadio, J.; Asakura, K. Chiral symmetry breaking in stirred crystallization of 1,1′-Binaphthyl melt. *J. Am. Chem. Soc.* **1999**, *121*, 1448–1451.
7. Ohno, O.; Kaizu, Y.; Kobayashi, H. *J*-aggregate formation of a water-soluble porphyrin in acidic aqueous media. *J. Chem. Phys.* **1993**, *99*, 4128–4139.
8. Ribó, J.M.; Crusats, J.; Sague, F.; Claret, J.; Rubires, R. Chiral sign induction by vortices during the formation of mesophases in stirred solutions. *Science* **2001**, *292*, 2063–2066.
9. Escudero, C.; Crusats, J.; Díez-Pérez, I.; El-Hachemi, Z.; Ribó, J.M. Folding and hydrodynamic forces in *J*-aggregates of 5-Phenyl-10,15,20-tris(4-sulfophenyl)porphyrin. *Angew. Chem. Int. Ed.* **2006**, *45*, 8032–8035.

10. Rossi, U.D.; Dähne, S.; Meskers, S.C.J.; Dekkers, P.J.M. Spontaneous formation of chirality in *J*-aggregates showing Davydov splitting. *Angew. Chem. Int. Ed. Engl.* **1996**, *35*, 760–763.
11. Yamaguchi, T.; Kimura, T.; Matsuda, H.; Aida, T. Macroscopic spinning chirality memorized in spin-coated films of spatially designed dendritic zinc porphyrin *J*-aggregates. *Angew. Chem. Int. Ed.* **2004**, *43*, 6350–6355.
12. Dzwolak, W.; Loksztejn, A.; Galinska-Rakoczy, A.; Adachi, R.; Goto, Y.; Rupnicki, L. Conformational indeterminism in protein misfolding: Chiral amplification on amyloidogenic pathway of insulin. *J. Am. Chem. Soc.* **2007**, *129*, 7517–7522.
13. Tsuda, A.; Alam, M.A.; Harada, T.; Yamaguchi, T.; Ishii, N.; Aida, T. Spectroscopic visualization of vortex flows using dye-containing nanofibers. *Angew. Chem. Int. Ed.* **2007**, *46*, 8198–8202.
14. Bloemendal, M.; van Grondelle, R. Linear-dichroism spectroscopy for the study of structural properties of proteins. *Mol. Biol. Rep.* **1993**, *18*, 49–69.
15. Adachi, K.; Watarai, H. Two-phase Couette flow linear dichroism measurement of the shear-forced orientation of a palladium(II)-induced aggregate of thioether-derivatised subphthalocyanines at the toluene/glycerol interface. *New J. Chem.* **2006**, *30*, 343–348.
16. Tsuda, A.; Nagamine, Y.; Watanabe, R.; Nagatani, Y.; Ishii, N.; Aida, T. Spectroscopic visualization of sound-induced liquid vibrations using a supramolecular nanofibre. *Nat. Chem.* **2010**, *2*, 977–983.
17. El-Hachemi, Z.; Arteaga, O.; Canillas, A.; Crusats, J.; Escudero, C.; Kuroda, R.; Harada, T.; Rosa, M.; Ribó, J.M. On the mechano-chiral effect of vortical flows on the dichroic spectra of 5-Phenyl-10,15,20-tris(4-sulfonatophenyl)porphyrin *J*-aggregates. *Chem. Eur. J.* **2008**, *14*, 6438–6443.
18. Yamamoto, T.; Tsuda, A. Vortex-induced alignment of a water soluble supramolecular nanofiber composed of an amphiphilic dendrimer. *Molecules* **2013**, *18*, 7071–7080.
19. Ando, Y.; Sugihara, T.; Kimura, K.; Tsuda, A. A self-assembled helical anthracene nanofibre whose *P*- and *M*-isomers show unequal linear dichroism in a vortex. *Chem. Commun.* **2011**, *47*, 11748–11750.
20. Tsujimoto, Y.; Ie, M.; Ando, Y.; Yamamoto, T.; Tsuda, A. Spectroscopic visualization of right- and left-handed helical alignments of DNA in chiral vortex flows. *Bull. Chem. Soc. Jpn.* **2011**, *84*, 1031–1038.
21. Wolffs, M.; George, S.J.; Tomovic, Z.; Meskers, S.C.J.; Schenning, A.P.H.J.; Meijer, E.W. Macroscopic origin of circular dichroism effects by alignment of self-assembled fibers in solution. *Angew. Chem. Int. Ed.* **2007**, *46*, 8203–8205.
22. Davidsson, Å.; Nordén, B.; Seth, S. Measurement of oriented circular dichroism. *Chem. Phys. Lett.* **1980**, *70*, 313–316.
23. Arteaga, O.; Escudero, C.; Oncins, G.; El-Hachemi, Z.; Llorens, J.; Crusats, J.; Canillas, A.; Ribó, J.M. Reversible mechanical induction of optical activity in solutions of soft-matter nanophases. *Chem. Asian J.* **2009**, *4*, 1687–1696.
24. Arteaga, O.; Canillas, A.; Crusats1, J.; El-Hachemi, Z.; Llorens, J.; Sacristan, E.; Ribo, J.M. Emergence of supramolecular chirality by flows. *Chem. Phys. Chem.* **2010**, *11*, 3511–3516.

25. El-Hachemi, Z.; Arteaga, O.; Canillas, A.; Crusats, J.; Llorens, J.; Ribo, J.M. Chirality generated by flows in pseudocyanine dye *J*-aggregates: Revisiting 40 years old reports. *Chirality* **2011**, *23*, 585–592.
26. Nordén, B.; Llndblom, G.; Jonás, I. Linear dichroism spectroscopy as a tool for studying molecular orientation in model membrane systems. *J. Phys. Chem.* **1977**, *81*, 2086–2093.
27. Rajendra, J.; Baxendale, M.; Rap, L.G.T.; Rodger, A. Flow linear dichroism to probe binding of aromatic molecules and DNA to single-walled carbon nanotubes. *J. Am. Chem. Soc.* **2004**, *126*, 11182–11188.
28. Nordén, B.; Elvingson, C.; Jonsson, M.; Åkerman, B. Microscopic behaviour of DNA during electrophoresis: Electrophoretic orientation. *Q. Rev. Biophys.* **1991**, *24*, 103–164.
29. Marrington, R.; Dafforn, T.R.; Halsall, D.J.; MacDonald, J.I.; Hicksa, M.; Rodger, A. Validation of new microvolume Couette flow linear dichroism cells. *Analyst* **2005**, *130*, 1608–1616.
30. Hicks, M.R.; Kowalski, J.; Rodger, A. LD spectroscopy of natural and synthetic biomaterials. *Chem. Soc. Rev.* **2010**, *39*, 3380–3393.
31. Nordén, B.; Rodger, A.; Dafforn, T. *In Linear Dichroism and Circular Dichroism: A Textbook on Polarized-Light Spectroscopy*; Royal Society of Chemistry: Cambridge, UK, 2010.
32. Nakamura, Y.; Aratani, N.; Osuka, A. Cyclic porphyrin arrays as artificial photosynthetic antenna: Synthesis and excitation energy transfer. *Chem. Soc. Rev.* **2007**, *36*, 831–845.
33. Shindo, Y.; Ohmi, Y. Problems of CD spectrometers. 3. Critical comments on liquid crystal induced circular dichroism. *J. Am. Chem. Soc.* **1985**, *107*, 91–97.
34. Van Gestel, J.; Palmans, A.R.A.; Titulaer, B.; Vekemans, J.A.J.M.; Meijer, E.W. "Majority-rules" operative in chiral columnar stacks of C_3-symmetrical molecules. *J. Am. Chem. Soc.* **2005**, *127*, 5490–5494.
35. Smulders, M.M.J.; Schenning, A.P.H.J.; Meijer, E.W. Insight into the mechanisms of cooperative self-assembly: The "sergeants-and-soldiers" principle of chiral and achiral C_3-symmetrical discotic triamides. *J. Am. Chem. Soc.* **2008**, *130*, 606–611.
36. Ghosh, S.; Li, X.-Q.; Stepanenko, V.; Würther, F. Control of H- and J-type π stacking by peripheral alkyl chains and self-sorting phenomena in Perylene bisimide homo- and heteroaggregates. *Chem. Eur. J.* **2008**, *14*, 11343–11357.
37. Albrecht, T.R.; Grütter, P.; Horne, D.; Rugar, D. Frequency modulation detection using high-Q cantilevers for enhanced force microscope sensitivity. *J. Appl. Phys.* **1991**, *69*, 668–673.
38. Fukuma, T.; Kimura, M.; Kobayashi, K.; Matsushige, K.; Yamada, H. Development of low noise cantilever deflection sensor for multienvironment frequency-modulation atomic force microscopy. *Rev. Sci. Instrum.* **2005**, *76*, 053704:1–053704:8.
39. Harada, N.; Takuma, Y.; Uda, H. The absolute stereochemistries of 6,15-dihydro-6,15-ethanonaphtho[2,3-c]pentaphene and related homologues as determined by both exciton chirality and X-ray Bijvoet methods. *J. Am. Chem. Soc.* **1976**, *98*, 5408–5409.
40. Harada, N.; Nakanishi, K. Exciton chirality method and its application to configurational and conformational studies of natural products. *Acc. Chem. Res.* **1972**, *5*, 257–263.
41. Iwaura, R.; Ohnishi-Kameyama, M.; Iizawa, T. Construction of helical *J*-aggregates self-assembled from a thymidylic acid appended anthracene dye and DNA as a template. *Chem. Eur. J.* **2009**, *15*, 3729–3735.

42. Smith, S.B.; Finzi, L.; Bustamante, C. Direct mechanical measurements of the elasticity of single DNA molecules by using magnetic beads. *Science* **1992**, *258*, 1122–1126.
43. Perkins, T.T.; Smith, D.E.; Larson, R.G.; Chu, S. Stretching of a single tethered polymer in a uniform flow. *Science* **1995**, *268*, 83–87.
44. Marko, J.F.; Siggia, E.D. Fluctuations and supercoiling of DNA. *Science* **1994**, *265*, 506–508.
45. Strick, T.R.; Allemand, J.-F.; Bensimon, D.; Bensimon, A.; Croquette, V. The elasticity of a single supercoiled DNA molecule. *Science* **1996**, *271*, 1835–1837.
46. Selvin, P.R.; Cook, D.N.; Pon, N.G.; Bauer, W.R.; Klein, M.P.; Hearst, J.E. Torsional rigidity of positively and negatively supercoiled DNA. *Science* **1992**, *255*, 82–85.
47. Bryant, Z.; Stone, M.D.; Gore, J.; Smith, S.B.; Cozzarelli, N.R.; Bustamante, C. Structural transition and elasticity from torque measurements on DNA. *Nature* **2003**, *424*, 338–341.
48. Baumann, C.G.; Smith, S.B.; Bloomfield, V.A.; Bustamante, C. Ionic effects on the elasticity of single DNA molecules. *Proc. Natl. Acad. Sci. USA* **1997**, *94*, 6185–6190.
49. Saminathan, M.; Antony, T.; Shirahata, A.; Sigal, L.H.; Thomas, T.; Thomas, T.J. Ionic and structural specificity effects of natural and synthetic polyamines on the aggregation and resolubilization of single-, double-, and triple-stranded DNA. *Biochemistry* **1999**, *38*, 3821–3830.